




Hard Anodizing of Aerospace AA7075-T6 Aluminum Alloy for Improving Surface Properties

Imran Ali¹ · M. M. Quazi²  · E. Zalnezhad³ · Ahmed A. D. Sarhan⁴ · N. Liana Sukiman¹ · M. Ishak²

Received: 4 February 2018 / Accepted: 6 June 2019 / Published online: 2 July 2019
© The Indian Institute of Metals - IIM 2019

Abstract In the current research work undertaken, an oxide film was grown by performing hard anodizing process on a pure aluminum layer deposited by PVD magnetron sputtering process on AA7075-T6 alloy. The corresponding tribo-mechanical properties were evaluated and compared with those of the base alloy. The dry sliding wear experiments were carried out to investigate wear resistance of anodized AA7075-T6 against the AISI SS316 counter-body by means of a reciprocating tribo-testing setup. The hardness of AA7075-T6 after the anodizing process exhibited an enhancement of about 1.94 times. Results revealed that the wear of anodized coating was exceptionally less when compared with the substrate. Based on morphology and chemistry changes of worn-out surfaces and debris, it was determined that severe abrasive and oxidative wear was the primary wear mechanism for AA7075-T6. The anodizing process increased the friction coefficient from 0.33 to 0.46 but reduced the wear severity by altering the wear mechanism into mild polishing and

abrasion. Anodizing enhanced the wear resistance of AA7075-T6 to about three times, and the wear rate decreased to around 4.3 times.

Keywords Anodizing · Wear resistance · AA7075-T6 alloy · Tribology · Hardness

1 Introduction

The applications of aluminum (Al) alloys in structural, automotive and aerospace applications have become omnipresent because of their high specific strength, corrosion resistance and ease of recyclability. With the advancements of the 7000 series of Al alloys, exceptional properties such as fatigue strength and fracture toughness have paved their way in replacing steel. In particular, various critical components made from AA7075 include aircraft fittings parts, gears and shafts, fuse parts, gears, meter shafts, keys, regulating valve parts and various aerospace components [1]. The Zn-based 7075 alloy exhibits constraints under dry sliding wear as they often experience severe wear damage primarily due to their comparatively low surface hardness and higher ductility [2]. Baydoğan et al. [3] and Cai et al. [4] have reported that AA7075-T6 alloy experiences severe wear under dry sliding conditions and, hence, is not a suitable candidate for applications wherein tribo-mechanical performance is prerequisite.

Countless efforts have been made in carrying out either modification of the bulk material [5], surface coatings [6] or by surface modifications [7]. Nevertheless, hard anodizing continues to remain a widely accepted surface coating method in which a thick and dense hard oxide layer can be grown by means of an inexpensive electrochemical

✉ M. M. Quazi
engrmoinquazi@gmail.com; moinquazi@ump.edu.my

✉ N. Liana Sukiman
nazatul@um.edu.my

Imran Ali
imran2016.um@gmail.com

¹ Department of Mechanical Engineering, Faculty of Engineering, University of Malaya, 50603 Kuala Lumpur, Malaysia

² Faculty of Mechanical Engineering, Universiti Malaysia Pahang, 26600 Pekan, Pahang, Malaysia

³ Biomechacin LLC., San Antonio, TX 78251, USA

⁴ Mechanical Engineering Department, King Fahd University of Petroleum and Minerals, Dhahran 31261, Saudi Arabia

process [8]. Anodic oxidation has been widely employed in enhancing the corrosion and wear resistance [9]. The applications of anodized products necessitate their usage in the ornamental, architectural and aerospace industries wherein hardness and wear resistance are of foremost importance in these applications [10].

Recently, Beri et al. [10] conducted a literature review on the mechanical properties of anodized Al and concluded that higher thickness of the coating could be formed with a decrease in solution temperature that would eventually produce wear-resistant coating. Gilbert et al. [11] studied the effect of stirring conditions on hard anodizing of AA6061-T6 and found that air bubbling stirring method exhibited uniform coating thickness. In another work by Lieu et al. [12], a surface hardness of 193 H_v corresponding to a coating thickness of 20 μm was obtained. The worn surface of anodized AA7075-T6 was characterized by mild scratching along with plastic deformation. Similarly, Roshani et al. [13] disclosed that by employing optimized pulse current, coatings registered a low friction coefficient of 0.35 under dry sliding conditions against alumina counter-body. However, it has been recorded that direct anodization of AA7075-T6 produces interfacial defects and brittle intermetallic which makes the substrate unfit for the treatment [14].

It is known that Al alloys containing silicon and copper tend to be porous and are not characterized to be harder when anodized [15]. Hence, one way to overcome this issue is to deposit a layer of pure Al on AA7075-T6 alloy by means of thin-film physical vapor deposition (PVD) technology and subsequently carry out a hard anodizing process. The objective of this research is to examine the coating characteristics and to consequently evaluate the tribological aspects of the anodized AA7075-T6 alloy by means of the aforesaid duplex process. The wear and friction coefficient of the substrate and coated sample shall be examined under dry sliding conditions in order to identify the extent to which the tribo-mechanical performance of AA7075-T6 is enhanced.

2 Experimental Details

2.1 Materials and Sample Preparation

The chemical composition of AA7075-T6 employed in this research work is (in wt%)—4.6 Zn, 1.8 Mg, 1.85 Cu, 0.06 Mn, 0.47 Si and 0.28 Cr. Samples of AA7075-T6 were cut in dimensions of 20 mm diameter and 5 mm thickness. For sample grinding, silicon carbide sandpapers with grit size ranging from 800 to 2200 were used. Subsequently, the samples were polished with 3- and 1-μm polycrystalline diamond suspended liquid solution (Buehler). After the

polishing process, the samples were cleaned ultrasonically in acetone for 15 min, degreased and dried out using nitrogen gas to prevent surface contamination.

2.2 PVD Coating Deposition and Anodizing Process

Metals with higher copper and silicon contents are difficult to be anodized [16]. Therefore, in order to cater to this problem, pure Al coated layer was deposited on the AA7075-T6 substrate by employing the PVD technique. The instrument for PVD magnetron sputtering used was an “SG Control Engineering Pte Ltd” system. The scheme of PVD machine included 600 W radio frequency (RF) and 1200 W direct current (DC) generators having the electrode dimensions of 4 × 12” that were 15 cm away from the target. The samples were placed on a substrate carrier, which was a circular rotatable plate. Next step was ion etching wherein Ar + sputtering was carried out in which the ions were accelerated by applying substrate bias potential against the samples. In this procedure, the chemisorbed nitrogen, oxygen and carbon atoms were subsequently evacuated. The deposition parameters for pure Al through PVD magnetron sputtering are given in Table 1.

After the deposition of pure Al layer, AA7075-T6 was put out for the electrochemical reaction of hard anodizing process. Hot solution of sodium hydroxide was utilized in order to etch the sample surfaces that would remove the minor surface imperfections. For hard anodizing process, ingredients, including sulfuric acid, phosphoric acid, carboxylic acid (1–10 carbon atoms), oxidizing inorganic acid and manganese (oxidized), were used to prepare the aqueous solution that will render the surface free from oxides. Eventually, the concentrated mixture of phosphoric and nitric acids was utilized to smoothen the surfaces chemically and to create a near-mirror finish. Following the cleaning process, the specimens coated with pure Al acted as anode that were taken in an electrolytic bath containing sulfuric acid. Thereafter, the current was delivered through the bath. For the hard anodizing process, a series of tests were carried out by varying voltage (10–40 V), temperature (0–25 °C), solution concentration (%) and time duration (30–90 min). Based on experiments performed, a 20 voltage, 10 °C temperature, 20% solution concentration and 30 min of anodizing process produced coatings with a hardness of 360 H_v. The sample with the highest hardness was subsequently tested for tribo-mechanical performance.

2.3 Dry Sliding Wear Test

Tribological tests were conducted under conditions of dry sliding by employing a high-frequency reciprocating friction monitor “DUCOM TR-282” designed to conform with the ASTM G133-05 standard specifications [17]. Wear

Table 1 PVD deposition parameters of pure Al coating

Coating	Evacuation pressure (Torr)	Sputtering pressure (Torr)	Deposition time (Hr)	DC power (W)	Temperature (°C)	DC bias voltage (V)
Al	2×10^{-5}	5.2×10^{-3}	6	350	200	75

resistance was examined by investigating the damage mechanism against a counter-body material of stainless steel. The cylindrical counter-body pin material was obtained from commercially obtainable AISI SS-316 annealed and cold-drawn stainless steel rod with composition as (wt%) C—0.8, Cr—16, Mn—2, Si—1, Mo—2, Ni—10 and Fe balance. The rod was mechanically turned in dimensions of 6 mm diameter and 8 mm length, cylindrical pins with a surface roughness of approximately $0.25 \mu\text{m}$ and an average measured surface hardness of around $240 H_v$. Three trials were conducted under normal load of 10 N and a reciprocatory amplitude stroke of 2 mm for 6 min along with the reciprocating frequency of 10 Hz. An average of five tests were carried out. For weight loss measurements, an analytical high precision weight balance “Denver Instrument” with accuracy of 0.1 mg was employed in order to compute the wear rates.

2.4 Characterization

The coating morphology, cross-sectional information and elemental compositions were examined by field emission scanning electron microscopy that was integrated with energy-dispersive X-ray spectroscopy (FESEM-EDS, FEI Quanta FEG 250). The hardness of the anodized layer was examined by Vickers micro-hardness measuring instrument “HMV Micro-Hardness Tester Shimadzu” furnished with Vickers indenter. The test duration was set to 20 s, and the normal load was 980.7 mN. In order to make sure that the hardness test results were reliable, 5 indentations were made through each sample surface and their average values were calculated. To examine the counter-body wear micrographs, Olympus BX51 light optical microscope was utilized and for micro-surface characterization (digital instruments) atomic force microscope (AFM) was utilized. The wear depth and surface roughness were measured with surface profilometry technique with the help of Mitutoyo Surftest Sv-2100.

3 Results and Discussion

3.1 Coating Features

In order to have a clear view of coating’s cross-sectional microstructure, FESEM imaging has been employed as

shown in Fig. 1. It is worth mentioning that the produced oxide layer formed by the anodizing process is very dense and harder than natural oxidation. Furthermore, the coating layers constituted by hard anodizing process increases the substrate surface melting point from approximately $650 \text{ }^\circ\text{C}$ to approximately $2000 \text{ }^\circ\text{C}$, which is higher enough to maintain the mechanical properties at the higher temperature as well. The SEM and EDX spot scan as illustrated in Fig. 1a show that $50\text{-}\mu\text{m}$ -thick Al_2O_3 is formed on the coating. Additionally, the 7075-T6 alloying elements are also present. Figure 1b presents the EDX line scan emanating from substrate to the end of the coating. The line scan indicates the reduction in concentration of Al and an increase in the concentration of O_2 as the scanner moves from the substrate to the coating. The interface between the coating and the substrate is free from defects, cracks or inclusions.

3.2 Coating Surface Hardness

The process parameter’s combinations for the highest surface hardness of the anodized coatings are voltage (20 V), temperature ($0 \text{ }^\circ\text{C}$), solution concentration (15%) and time (120 min). The confirmation tests have been carried out as well to corroborate the best condition results attained for surface hardness. By applying the above-mentioned parameters levels, the optimum hardness value of $340 H_v$ is obtained. When compared with the hardness of base alloy ($175 H_v$), an increase in the hardness of about 94.2% is observed after the anodizing process. Roshani et al. [13] employed pulse direct current for their anodization process of AA1050 and obtained a higher value of surface hardness to about $440 H_v$.

3.3 Wear Rate and Friction Coefficient

The kinetic friction coefficient “ μ_k ” versus time curves for substrate and anodized AA7075-T6 under normal load of 10 N are depicted in Fig. 2a, b, respectively. The values of the kinetic friction coefficient have been calculated depending on root mean square given on instrumentation output. The acquired average value from the plotted friction coefficient with respect to cumulative time graphs report the friction coefficient values of uncoated AA7075-T6 and anodized surface as 0.32 and 0.47, respectively. As it is apparent, the coefficient of friction for the anodized

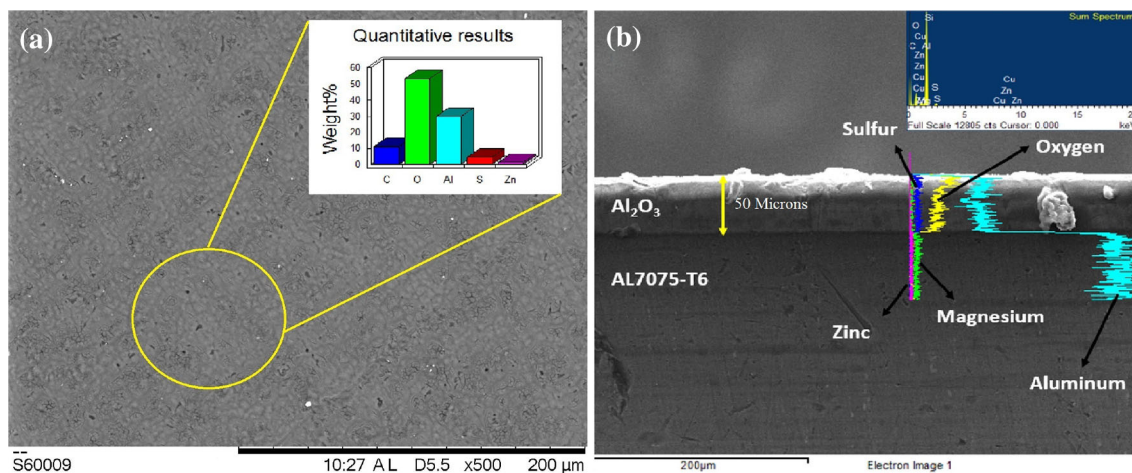
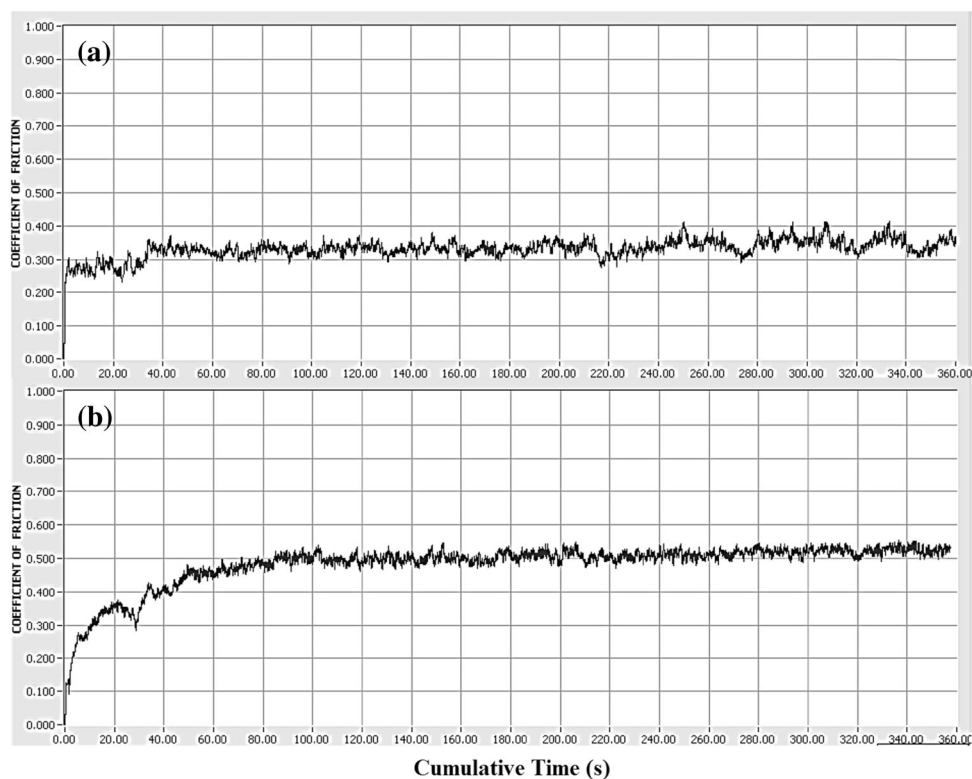


Fig. 1 Scanning electron micrograph and EDX **a** area scan on anodized AA7075-T6 surface and **b** line scan on coating/substrate cross section

Fig. 2 Friction coefficient versus cumulative time for **a** AA7075-T6 and **b** anodized AA7075-T6



sample is 30% higher than the uncoated bulk substrate. Similar friction coefficient for the wear of anodized coatings against stainless steel has been reported by Kim, Hyo-sang, et al. [18]. In a recent work by Roshani et al. [13], the friction coefficient of anodized AA1050 is obtained as between 0.35 and 0.48. Liew et al. [12] stated that the larger values of friction coefficient result in higher energy dissipation that may be detrimental to the mechanical efficiency of the system.

The mutual characteristic present in friction diagrams is that, initially the wearing of surface asperities occurs. In

general, “ μ_k ” increases sharply at the beginning, reaching the steady-state condition in a short period. This phenomenon is defined as “initial successive wear” of surface micro-asperities and the better conformism of wear scars. In the initial stages, the wear is instigated by brittle micro-fractures within surface grains. This is in the later stages followed by tribo-chemical reactions [19]. Table 2 summarizes the results of friction and wear rate for AA7075-T6 and anodized coating. The calculated wear loss for anodized samples is approximately 4.3 times lesser than that of AA7075-T6 alloy. The specific wear rate is calculated by

Table 2 Results of pin-on-disk wear test of the aluminum alloy with and without the coating produced by anodizing with SS316 Steel

Specimen	Hardness (H _v)	Roughness before wear (nm)	Roughness after wear (nm)	Friction coefficient	Wear depth (um)	Wear loss (mm ³ min ⁻¹)	Specific wear rate (mm ³ N m ⁻¹)
AA7075-T6	175	19.06	172.2	0.33	7	4.83 × 10 ⁻²	4.14 × 10 ⁻³
Anodized coating	340	8.9	14.735	0.47	2.35	1.15 × 10 ⁻²	9.60 × 10 ⁻⁴

keeping in view the density of the coating to be 3.0 mg m⁻³.

3.4 Characterization of Worn Surfaces

It is understood that the substrate has undergone extensive plowing, with visible scars, grooves along with craters. Additionally, a change in depth as the wear progresses can also be noticed. Besides, in the matter of anodized AA7075, the coating does not wear or peel off and the substrate is not revealed during the course of the wear testing. Such wear characteristics suggest the integrity of the anodization process in protecting the substrate. When viewed from the micro-asperities' aspect, the SEM and EDX spectrum analysis of wear scars of the coatings and substrate have been carried out at various sections to investigate the wear modes (Fig. 3). Figure 3 illustrates the top view morphology of the substrate and their corresponding wear tracks. Within the selected experimental conditions, the tribological test exhibits a contrasting difference in the wear characteristics of the substrate and coatings. Mainly, more than one single wear mechanism

occur at the same instance, whereas for dry-sliding-based wear test, the scar comprises of rough grooves and smeared segments. Various inferences can be interpreted by detecting different groove widths and depths under similar loads that indicate discrepant wear mechanisms. Figure 3a shows wider grooves and scars together with material pullout and visible cracks (Fig. 3b) on the surface of AA7075. The material pullout can be attributed to fatigue cracks occurring as a result of repeated cyclic stress larger than the material's yield strength [20].

The wear mode of the uncoated Al alloy proceeded by both oxidative and abrasive modes as per simultaneous inferences are made from SEM and EDX (Fig. 3c). Greater concentrations of iron implies that the material is transferred from the pin thereby, taking part in faster removal of material. As it is depicted in Fig. 3b, severe plastic deformation is also accompanied by plowing and smearing. The wear of anodized Al is characterized by the tribo-polishing mechanism that is characterized by the absence of any such kind of plowing or severe plastic deformation (Fig. 3d). The wear can be considered as mild oxidative wear along with some concentration of Al and oxygen

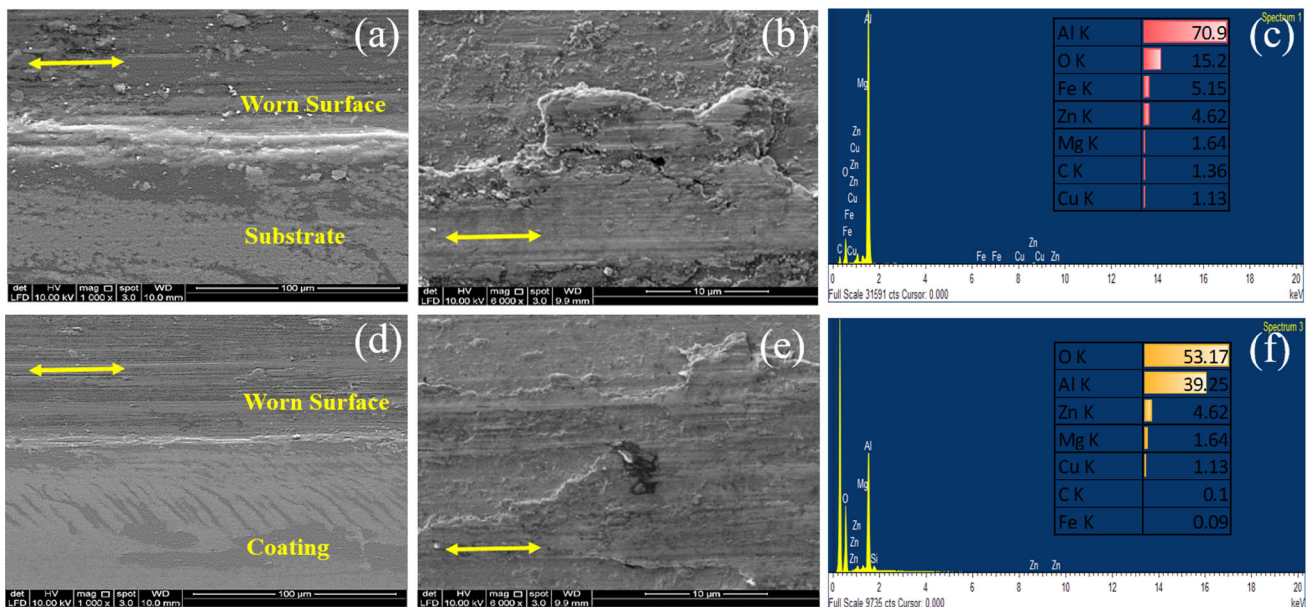


Fig. 3 Scanning electron micrograph and EDX spot scan of worn scars for **a–c** AA7075-T6 and **d–f** anodized AA7075-T6

present in the phases. This is supported by EDX, showing oxygen in higher concentrations while some of the traces of worn-out iron is also present (Fig. 3f). Sabitini et al. [21] in their work of spark anodization have grown Al_2O_3 on AA7075 and found that the dry sliding wear testing exhibits contrasting wear mechanisms. The coating exhibits predominant abrasion due to higher hardness and three bodies rolling. Secondary wear mechanisms have been identified to be tribo-oxidation leading to material transfer on the counter-face. Some authors [13, 21] also found cracks in their SEM of worn scars; however, this is not the case in our study.

3.5 Characterization of Counter-Bodies and Wear Debris

Typical optical microscopic images of the degraded counter-bodies of AA7075 and anodized AA7075 are portrayed in Fig. 4, respectively. The width and morphology of the scars are appropriate criteria to examine the severity and mode of wear. It must be mentioned that the scar width is calculated based on averaged values taken sequentially along the scar's length. The tracks on the AA7075-T6 scar (Fig. 4a) are found to be shiny because of the degradation of the outer pin surface, thereby disclosing the fresh steel subsurface. Similarly, for the case of the anodized counter-body pin (Fig. 4b), marks with oxidized transferred material are present. This explicit blackish area is considerably in contrast with unworn pin surface, supporting the material transfer from the anodized layer to their counterpart pins. The counter-body wearing against harder anodized coating experiences greater wear translating into an average width of $643\ \mu\text{m}$ scar width when compared with AA7075 counter-body having approximately $314\ \mu\text{m}$ scar width. Liew et al. [12] in their work summarized that the alumina coating causes rapid wear of the counter-face material.

Figure 5 depicts the general characteristics of worn debris that is generated during tribological wear. The ductile AA7075-T6 debris exhibits more of larger sized particles as a result of severity in wear (Fig. 5a). These particles exhibit a greater tendency to agglomerate. The amount of agglomeration is found to be lesser with a smaller particle size from anodized coating (Fig. 5c). The crack's initiation on the surface is the starting point of debris generation and transfer layer formation. For the case of uncoated Al alloy, the fracture toughness is the main mechanical property controlling wear rate instead of hardness, providing the Al alloy with lesser resistance to pullout or detach, thereby exhibiting adhesive wear as visible on counter-body of AA7075-T6 (Fig. 4a). The intense tribological load causes extrusion of the chunks trapped during the tribological testing process, which are visible in Fig. 5b. The debris of coated AA7075-T6 is, in general, more oxidative, irregular shaped and comprising of finer particles indicating that the wear has progressed through oxidative mode. In contrast, the wear of AA7075-T6 is found to have progressed as adhesive, abrasive mode with severe plastic deformation being involved. Anodization process reduces the amount of adhesion by generating lesser quantity and size of the debris [10]. Kim et al. [18] in their research work on nano-porous anodic alumina have shown that the worn-out particles are micro-cylinder shaped due to the repeated rolling of microparticles. However, for the substrate that does not resist plastic deformation, plate-like particles are generated due to delamination of tribo-layers under repeated cyclic fatigue.

3.6 Changes in Surface Morphologies

The change in surface morphology by virtue of the wear process leads to material removal that can be detected by the AFM technique. AFM is used in contact mode to determine surface texture and topographical

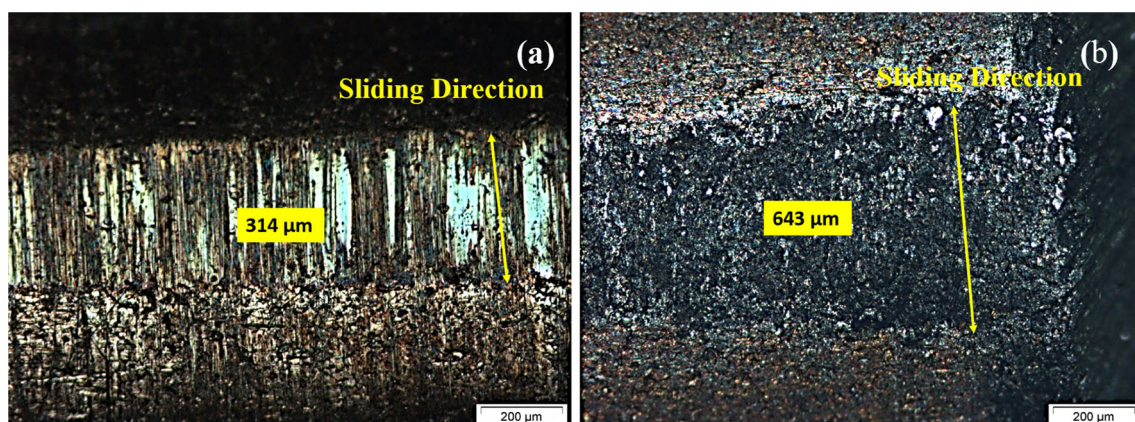


Fig. 4 Degraded counter-bodies for **a** AA7075 and **b** anodized AA7075

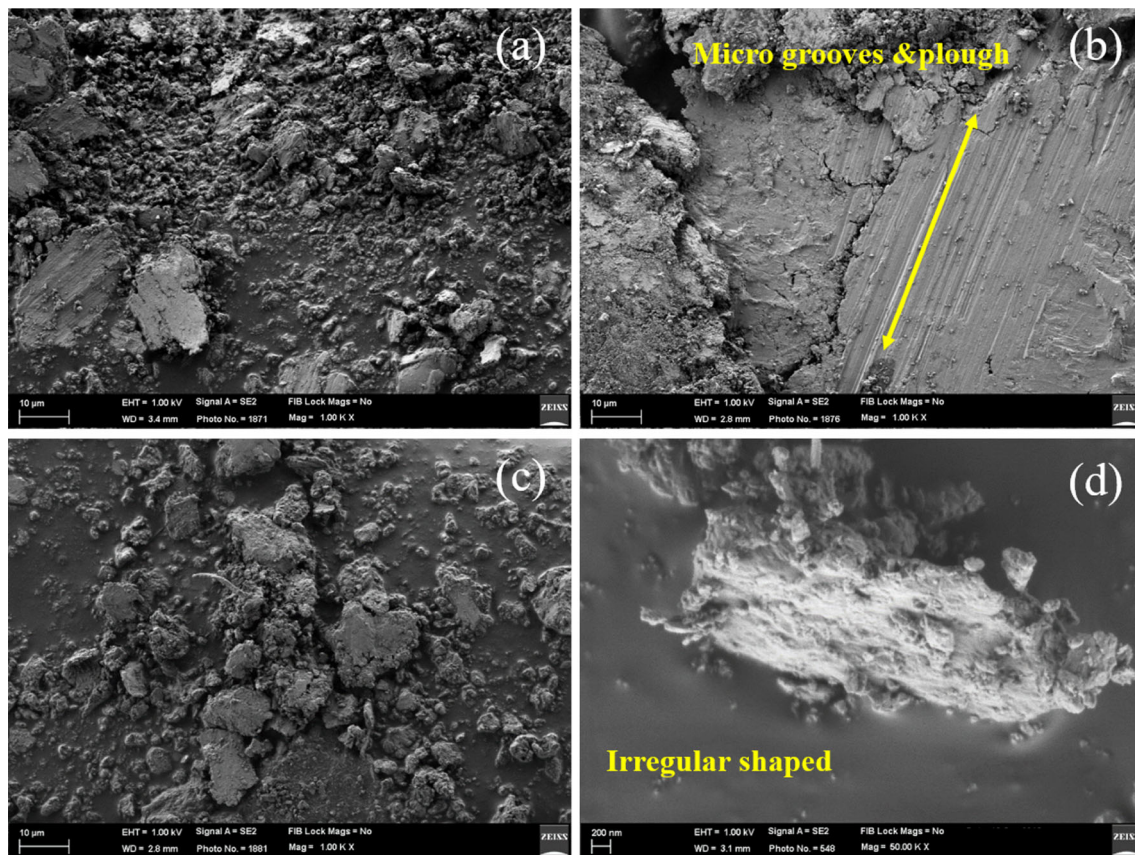


Fig. 5 Wear debris for **a, b** AA7075 and **c, d** anodized AA7075

characterization. The most frequently measured roughness parameter is R_a , which is calculated based on the roughness average of surfaces microscopic peaks and valleys. Figure 6 represents the 3D-AFM images acquired for uncoated and coated samples before and after the wear testing. The AFM images have been taken over an area of $30\ \mu\text{m} \times 30\ \mu\text{m}$. As observed in Fig. 6b, there are no visible surface defects in the form of craters or microparticles present on the coated samples. For the case of the AA7075-T6 sample, Fig. 6a shows the existence of grooves formation, which is enclosed with higher peaks. These peaks lead to the formation of grooves as a result of plastic deformation. Specifically, in the case of Al alloys, the wear takes place by homogeneous deformation in an isothermal mode whereby the material is removed by extrusion and the coatings peel off from the substrate because of the shearing of the material [18]. The average roughness values inside the wear tracks of the substrate and anodized specimens are 172.2 nm and 14.73 nm, respectively, whereby anodized samples are accounted for a minimum of 11.7 times lesser R_a than the former. This observation confirms the role of anodization in reducing the friction and wears that is postulated to be the main reason for such a significant difference. Correspondingly, the arithmetic average surface

roughness of substrate and coatings is also evaluated. The changes in surface roughness of AA7075-T6 substrate from 19.06 nm to that of 172.2 nm after wear show a significant increase when compared with the anodized substrate. The anodized Al registers a change in roughness value from 8.9 nm to that of 14.73 nm.

Figure 7a, b illustrates the 3D surface scan and surface profilometry to indicate the wear depth for the substrate and coating, respectively. The coatings profilometry scan displays two sharp endings at the edges of tracks which are due to shearing that has occurred during tribo-chemical wear process [22]. During the shearing process, the reciprocating pin pushes the material sideways at the two extreme ends to form such wear contour, inducing compressive force leading to the emanation of such sharp edges. From the surface profilometry of samples across the scars, the maximum groove depth between peak and valleys inside wear scar between pileups is found to be approximately $7\ \mu\text{m}$ for AA7075-T6 that is followed by $2.35\ \mu\text{m}$ for anodized Al which is about three times lesser. As depicted earlier, as the surface hardness is improved, friction coefficient increases due to the porous nature of the coating. However, the surface roughness after wear is indicative of micro-polishing and lesser wear depth points

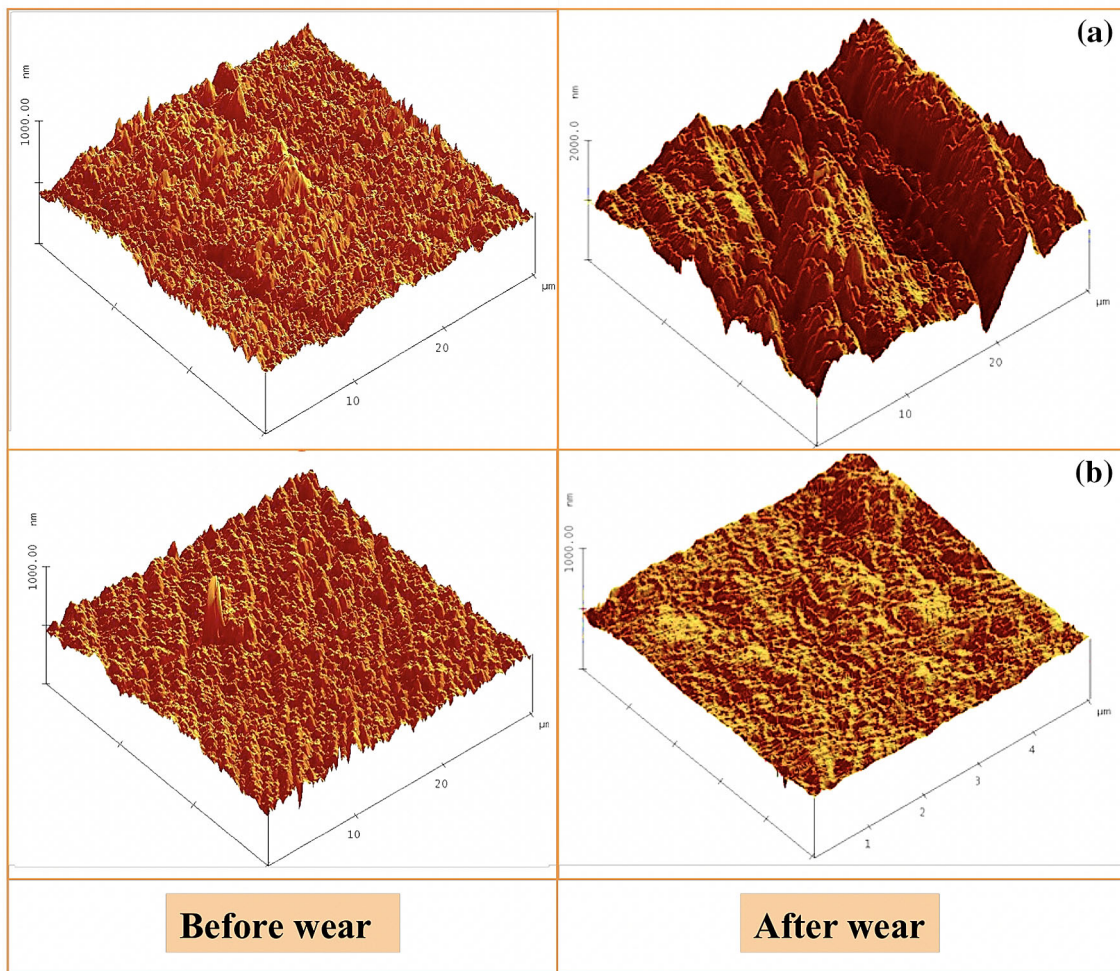


Fig. 6 Surface morphologies and roughness for **a** AA7075-T6 and **b** anodized AA7075-T6

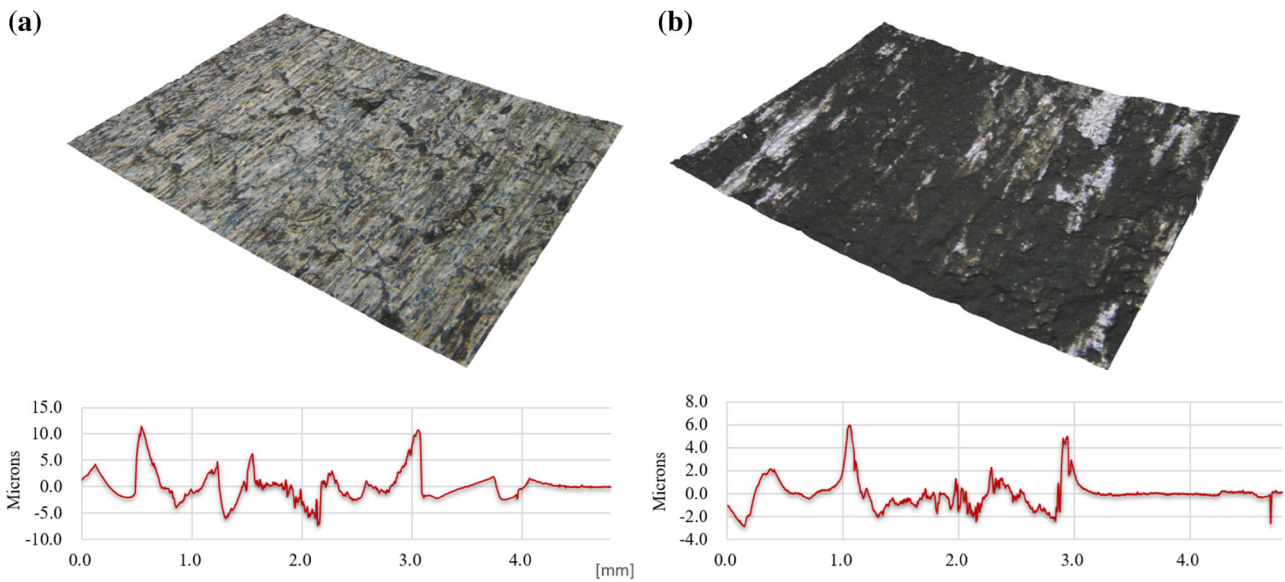


Fig. 7 3D surface texture and surface profilometry of the worn surface of **a** AA7075-T6 and **b** anodized AA7075-T6

toward better wear resistance of the coating. The anodizing experiments lead to an increase in hardness of AA7075 to about 1.94 times. In a research work carried out by Bozza et al. [14], a maximum hardness of 370 H_v is obtained when using direct current of 24 mA/cm² for 95 min to anodize AA7075.

4 Conclusions

In the current research work undertaken, AA7075-T6 was anodized with the aid of a pure Al layer that was deposited by PVD magnetron sputtering technique. Anodization of this layer was performed by varying the parameters like temperature, voltage, time duration and solution concentration. The following conclusion could be drawn from this work:

1. The parameter's combination for the best surface hardness of the anodized coating was voltage (20 V), temperature (0 °C), solution concentration (15%) and time (120 min).
2. Anodizing resulted in an improvement in the hardness of AA7075-T6 by about 1.94 times. Wear testing revealed severe grooving on AA7075-T6 resulting in wider and deeper plows along with plate-like debris onto which smaller particles were agglomerated. The wear analysis revealed the transition from mild to severe wear, which characterized the combination of oxidative, adhesive and abrasive wears mechanisms. Contrastingly, the anodized surface under the tribo-wear experiment was merely tribo-polishing without any distinct observations of visible surface plowing or groove formation which specified milder wear. The wear rates of anodized samples were about 4.3 times lesser than the substrate AA7075-T6.
3. The dry sliding wear of AA7075-T6 exhibited a friction coefficient value of 0.33. Due to induced porosity created by the anodization process, an increase of 31% friction coefficient was witnessed. Based on surface profilometry, the maximum wear depth observed was three times lesser reported for anodized Al contributing to 66.4% decrease in the wear of AA7075-T6.

Acknowledgements This research work is funded by the University Malaya (UM) Research Grant (UMRG) Grant RP032C-15AET, and FP055-2015A from the Ministry of Higher Education, Malaysia. This work was also funded by UM Grant No PG179-2016A. We would like to acknowledge financial support from the Ministry of Education

Malaysia (Research Grant Project No. RDU1803171) through the Universiti Malaysia Pahang.

Compliance with Ethical Standards

Conflict of interest The authors report no conflict of interests.

References

1. Hui W, Luo Y-b, Friedman P, CHEN M-h, and Lin G, *Trans Nonferrous Metals Soc China* **22** (2012) 1.
2. Zhang T, and Li D, *Wear* **251** (2001) 1250.
3. Baydoğan M, Çimenoglu H, and Kayalı E S, *Wear* **257** (2004) 852.
4. Cai Z-B, Zhu M-H, and Lin X-Z, *Trans Nonferrous Metals Soc China* **20** (2010) 371.
5. Dutkiewicz J, and Litynska L, *Mater Sci Eng A* **324** (2002) 239.
6. Quazi M M, Ishak M, Arslan A, Nasir Bashir M, and Ali I, *J Adhes Sci Technol* **32** (2018) 625.
7. Arslan A, Masjuki H H, Kalam M A, Varman M, Mosarof M H, Mufti R A, Quazi M M, Khuong L S, Liaqat M, Jamshaid M, Alabdulkarem A, and Khurram M, *Surf Coat Technol* **322** (2017) 31.
8. Han B, Zal Nezhad E, Musharavati F, Jaber F, and Bae S, *Coatings* **8** (2018) 459.
9. Chelliah N M, Saxena A, Sharma K, Singh H, and Surappa M, *Surf Interfaces* **7** (2017) 139.
10. Beri R, Kushwaha M K, and Grover N, *A Review on Studies of Mechanical Properties of Anodized Alumina Oxide* (2017).
11. Gilbert F, Dube D, Ghali E, and Tremblay R, *Can Metall Q* **53** (2014) 381.
12. Liew K W, Chia S Y, Kok C K, and Low K O, *Mater Des* **48** (2013) 77.
13. Roshani M, Rouhaghdam A S, Aliofkhaezraei M, and Astarae A H, *Surf Coat Technol* **310** (2017) 17.
14. Bozza A, Giovanardi R, Manfredini T, and Mattioli P, *Surf Coat Technol* **270** (2015) 139.
15. Sarhan A A, Zalnezhad E, and Hamdi M, The influence of higher surface hardness on fretting fatigue life of hard anodized aerospace AL7075-T6 alloy. *Mater Sci Eng A* **560** (2013) 377.
16. Kelly P, Abu-Zeid O, Arnell R, and Tong J, *Surf Coat Technol* **86** (1996) 28.
17. ASTM G, 133-05. *Standard Test Method for Linearly Reciprocating Ball-on-Flat Sliding Wear, Annual Book of ASTM Standards* (2005), p 3.
18. Kim H-s, Kim D-h, Lee W, Cho SJ, Hahn J-H, and Ahn H-S, *Surf Coat Technol* **205** (2010) 1431.
19. Wang Y, Xia L, Ding J, Yuan N, and Zhu Y, *Tribol Lett* **49** (2013) 431.
20. Camargo A, and Voorwald H, *Fatigue Fract Eng Mater Struct* **30** (2007) 993.
21. Sabatini G, Ceschini L, Martini C, Williams JA, and Hutchings IM, *Mater Des* **31** (2) 816.
22. Kato K, *Proc Inst Mech Eng Part J J Eng Tribol* **216** (6) 349.

Publisher's Note Springer Nature remains neutral with regard to jurisdictional claims in published maps and institutional affiliations.